Int. J. Multiphase Flow Vol. 18, No. 6, pp. 965–976, 1992
Printed in Great Britain.

0301-9322/92 $5.00 + 0.00

PROPAGATION CHARACTERISTICS OF PRESSURE DISTURBANCES ORIGINATED BY GAS JETS IN FLUIDIZED BEDS

D. MUSMARRA,[1] S. VACCARO,[2] M. FILLA[3] and L. MASSIMILLA[1]

[1]Dipartimento di Ingegneria Chimica, Università di Napoli "Federico II" e Istituto di Ricerche sulla Combustione, CNR, P. le V. Tecchio, 80125 Napoli, Italy

[2]Dipartimento di Chimica, Università, via Mezzocannone 4, 80134 Napoli, Italy

[3]Istituto di Chimica Industriale, Università, via Marzolo 9, 35131 Padova, Italy

(Received 1 October 1991; in revised form 15 July 1992)

Abstract—An experimental investigation has been carried out on velocities and amplitudes of pressure disturbances in fluidized beds made of 100–200 μm glass ballotini. Disturbances were originated by gas jetting in a 0.35 m i.d. fluidized bed. A fluidization tube 0.10 m i.d. has also been used. Different types of disturbances have been induced in the bed contained in this tube: injection of a freely rising bubble and of a captive bubble; injection of a bubble chain; and compression of the bed free surface. The dynamic wave character of the disturbances has been shown. Velocities and amplitudes of waves moving through the beds have been measured. In particular, wave velocities have been compared with theoretical results obtained by the application of "pseudo-homogeneous" and "separated phase flow" models.

Key Words: fluidization, gas jets, pressure fluctuations, dynamic waves

1. INTRODUCTION

Gas discharge through a nozzle into a fluidized bed gives rise to a number of phenomena. They include the detachment of bubbles at the tip of a jet-like void, the expansion and contraction of the jetting region and the motion of solids throughout the bed (Massimilla 1985). Pressure fluctuations related to these phenomena, which often reach the level of local average bed pressures, affect the mass and heat exchange between the jet and the surrounding dense phase significantly (Filla *et al.* 1986; Vaccaro *et al.* 1989).

Previous works (Filla *et al.* 1986; Lirag & Littman 1971; Fan *et al.* 1981; Roy *et al.* 1990) have examined the propagation of pressure disturbances in fluidized beds by multipoint simultaneous measurements of pressure. These analyses were based on instantaneous pressures, i.e. on the pressures recorded at the same instant at different locations in the bed. Propagation velocities in the range 5–45 m/s are reported in these works (table 1).

The present study shows, however, that the results of multipoint simultaneous pressure measurements should be interpreted with caution in the case of gas jetting in a relatively large diameter fluidized bed. Difficulties in determining the direction and velocity of propagation are due to uncertainties about the location of the source of pressure fluctuations within the jetting region, the occurrence of local disturbances associated with bubble coalescence and splitting, and attenuation of disturbances travelling through heterogeneous mixtures made of dense phase and bubbles.

With this in mind, two apparatus have been used in the present work: a main pre-pilot scale apparatus operated with fluidized beds, in which pressure disturbances were generated by gas jetting; and a supplementary small-scale apparatus containing fluidized beds, in which disturbances were induced by controlled external sources.

The propagation velocities of the disturbances measured in the two columns are compared with each other and with predictions from available theories. Changes in amplitude of the pressure disturbances travelling radially and vertically through the bed are also determined. Altogether, the relevance of these results goes beyond the interaction between jets and fluidized beds. It may extend, among others, to the study of the propagation of dynamic waves in two-phase media. These waves, together with continuity waves (Wallis 1969, chap. 6), play a role in the stability of homogeneously

Table 1. Propagation velocities of pressure disturbances in fluidized beds reported in the literature

Authors	Measured velocities [m/s]	Direction of propagation	Bed materials	Major aim of the study
Lirag & Littman (1971)	7	Downward	Glass beads, 500, 318 and 218 μm average diameter	Bubbling phenomena
Fan et al. (1981)	45	Downward	Sand, 500 and 700 μm average diameter	Bubbling phenomena
	5	Upward		
Filla et al. (1986)	17.5–11	Radial	Silica sand, 200–400 μm	Jet–fluidized bed interactions
	6–10–8.5	Upward		
Roy et al. (1990)	10–20	Downward and upward	Several materials with different density and diameter	Propagation of sound waves in fluidized beds

fluidized beds (Wallis 1962; Verloop & Heertjes 1970; El-Kaissy & Homsy 1976; Mutsers & Rietema 1977; Foscolo & Gibilaro 1984).

2. EXPERIMENTAL

The Main Apparatus

This apparatus is made of a perspex cylindrical column 0.35 m i.d. and 2 m high (figure 1). It is equipped with an axial upward discharging nozzle 0.025 m dia flush with a perforated plate distributor whose 0.6 mm holes are arranged in a 2 mm square pitch. Two vertically aligned pressure taps are located at the column wall, 0.06 and 0.18 m above the gas distributor. An axial probe, made of a 1.0 mm o.d. tube, is located 0.06 m from the bed bottom. Four 0.3 mm radial holes are drilled on the lateral surface of the probe 5 mm from the tip. The bed was made of

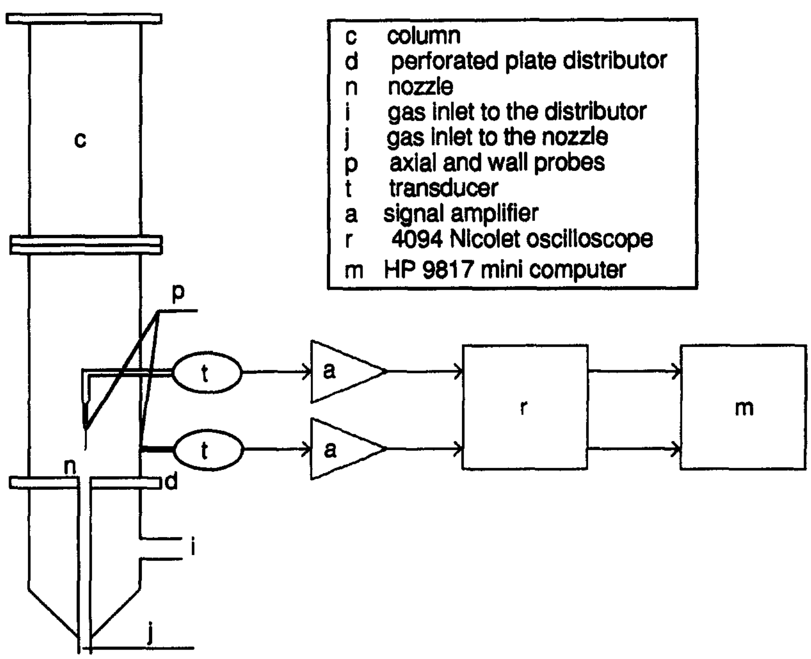

Figure 1. 0.35 m i.d. column with an axial upward discharging 0.025 m nozzle in the center of a perforated plate distributor.

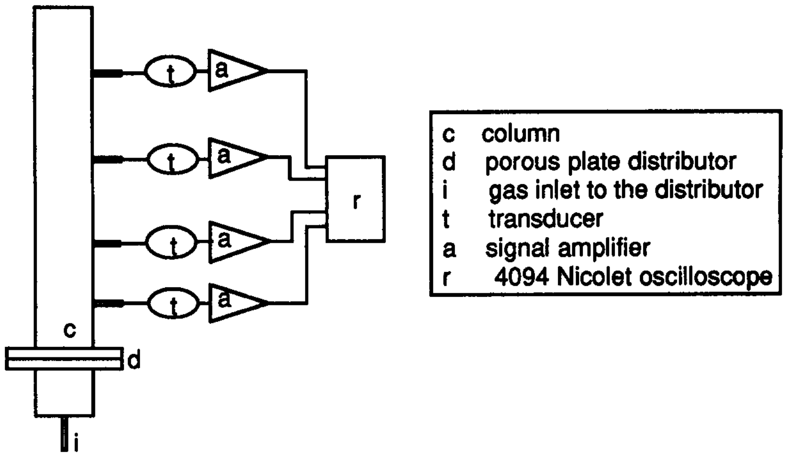

Figure 2. 0.10 m i.d. experimental apparatus.

100–200 μm glass ballotini whose density ρ_p was 2600 kg/m^3, the minimum fluidization velocity $U_{mf} = 0.021$ m/s and the minimum bubbling velocity $U_{mb} = 0.026$ m/s. The static bed height was 0.3 m. Fluidization velocities at the distributor U were in the range 0.026–0.049 m/s; jet velocities u_j were 17.5 and 35 m/s.

Propagation velocities of disturbances naturally generated by gas discharge through the jet nozzle have been determined by measuring simultaneously instantaneous pressures at two locations in the bed. As shown in figure 1, the column was instrumented to record and process the pressure disturbances induced by jetting.

The Supplementary Apparatus

This apparatus is made of a perspex cylindrical column 0.10 m i.d. and 1.2 m high (figure 2). It is equipped with a porous plate gas distributor and with 10 vertically aligned equally spaced pressure taps drilled in the wall. The same 100–200 μm glass ballotini used in the experiments with the main apparatus were charged in the column of the supplementary apparatus. The static bed height was 1.05 m. The bed was operated at velocities U between U_{mf} and U_{mb}, and also above U_{mb}.

The column was instrumented to record and process both impulsive and periodic disturbances. Impulsive disturbances were imparted to the bed by compressing the free surface with a

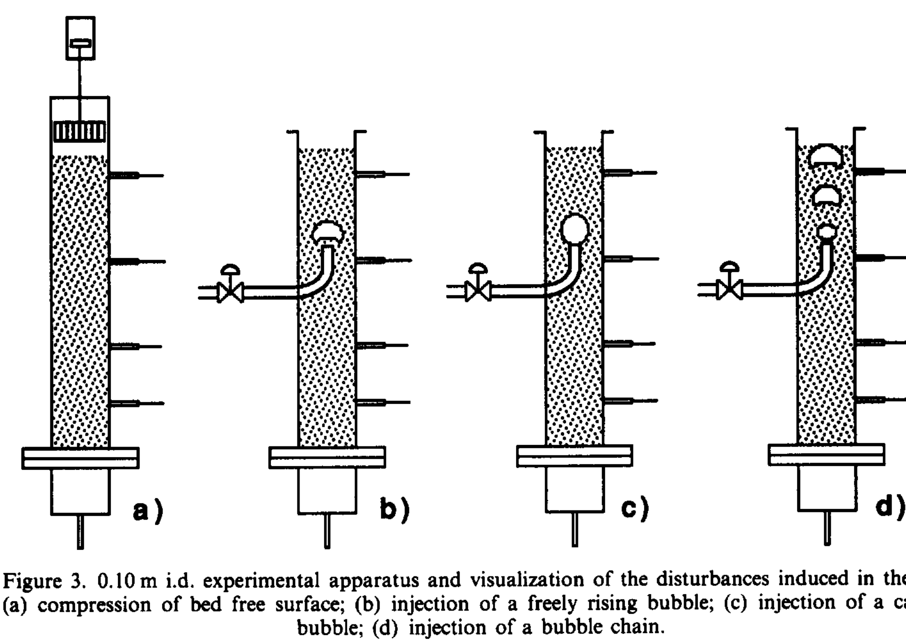

Figure 3. 0.10 m i.d. experimental apparatus and visualization of the disturbances induced in the bed: (a) compression of bed free surface; (b) injection of a freely rising bubble; (c) injection of a captive bubble; (d) injection of a bubble chain.

pneumatically operated gas permeable piston [figure 3(a)], by injecting a single gas shot which gave a freely rising bubble [figure 3(b)] and by injecting a single gas shot which gave a captive bubble anchored at the nozzle by a gas tight elastic membrane [figure 3(c)]. The periodic disturbance was generated by forcing a bubble chain through a vertical nozzle [figure 3(d)]. Pressure measurements were always made in the undisturbed section of the bed below the origin of the disturbance under all these conditions. Pressure signals were measured above as well as below the source of the disturbance under the conditions shown in figure 3(b).

Processing of Experimental Data

The data acquisition system includes Schaevitz P502 strain-gauge pressure transducers, signal amplifiers and a Nicolet 4094 digital oscilloscope and recorder. Each record consists of about 8000 point values, which in the case of periodic disturbances were processed off-line on an HP 9817 minicomputer.

The propagation velocities of disturbances (c) have been obtained as the ratio of the distance between two probes to the time delay between the corresponding pressure–time signals. The time delay between two points at a known distance (one at the wall and the other on the axis or both at the wall) has been determined by means of cross-correlation for periodic disturbances or by direct inspection of records for impulsive disturbances.

The amplitude of periodic pressure disturbances (A_p) has been calculated by means of the relationship

$$A_p = \sqrt{\sum_1^N \frac{[P(t) - P_{av}]^2}{N}},$$

$P(t)$ and P_{av} being the instantaneous and average pressure values, and N the number of point values. The amplitude of impulsive pressure disturbances (A_s) has been obtained as the difference between the maximum of the pressure–time record and the baseline pressure determined by the gas pressure drop through the bed in the absence of disturbances.

3. RESULTS

Propagation Velocity of Pressure Disturbances

Typical pressure profiles determined on the axis and at the wall 60 mm above the distributor in the 0.35 m i.d. column with jet are shown in figure 4. Periodic pressure disturbances originated by jets proceed from the center of the 0.35 m i.d. column toward the wall, and from the base toward the top of the bed. Pressure signals at the wall are delayed with respect to those at the axis and the delay increases with distance from the gas distributor. With reference to the experimental

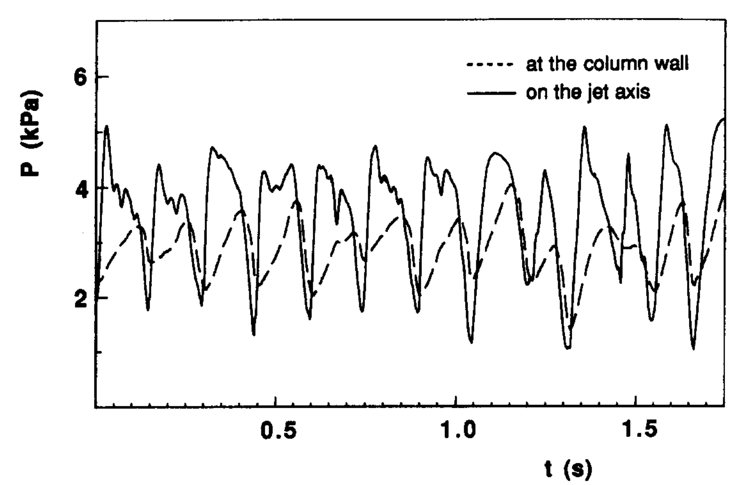

Figure 4. 0.35 m i.d. column. Typical pressure records 60 mm above the distributor ($U = 0.026$ m/s; $u_j = 35$ m/s).

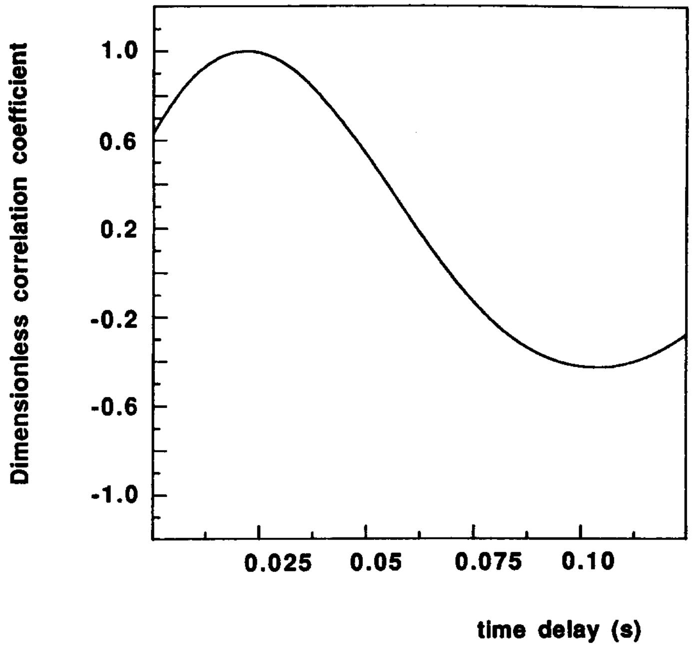

Figure 5. 0.35 m i.d. column. Cross-correlation diagram of the pressure profiles in figure 4.

conditions of figure 4, the time delay of the signal at the wall with respect to that on the axis is obtained by the cross-correlation diagram in figure 5, which shows that the most probable time delay is about 0.022 s. Correspondingly, the velocity of propagation of the disturbance $c = 8.6$ m/s.

Propagation velocities of disturbances obtained with the 0.35 m i.d. column under various experimental conditions are reported in table 2. They range between 6 and 16 m/s. Neither u_j nor U seem to influence c when the probes are located on the axis and at the wall. On the contrary, u_j and U affect this velocity significantly if the probes are both at the wall. As observed in section 1, uncertainties about the actual location of the source of the disturbance might explain this discrepancy.

Typical pressure profiles determined with the 0.1 m i.d. column at the same bed expansion ϵ_{mb} in response to piston step compression, injection of a single freely rising bubble, injection of a captive bubble and bubble chain are reported in figures 6–9. The diagrams shown in these figures give directly, for each external disturbance to which they refer, the time delays of the onset of the disturbance at various heights above the distributor. The propagation velocities c, corresponding to the three experimental arrangements, are 21, 19 and 17.8 m/s, respectively. The time delay between periodic signals in figure 9 is obtained by the cross-correlation plot in figure 10. The propagation velocity is 15.5 m/s in this case.

Values of c obtained with the 0.1 m i.d. column under various experimental conditions are reported in table 3. It appears that:

(i) At $U < U_{mb}$, propagation velocities increase as the dense phase voidage decreases

(ii) At $U > U_{mb}$, the propagation velocity is not appreciably affected by the presence of bubbles

Table 2. Propagation velocities (m/s) measured with the 0.35 m i.d. column ($U_{mf} = 0.021$ m/s; $U_{mb} = 0.026$ m/s)

U[m/s] / u_j[m/s]	0.026		0.049	
	a	b	a	b
17.5	8.0	10.9	8.3	6.1
35.0	8.6	16.1	8.0	11.6

[a]A probe on the axis and one at the wall.
[b]Both probes at the wall.

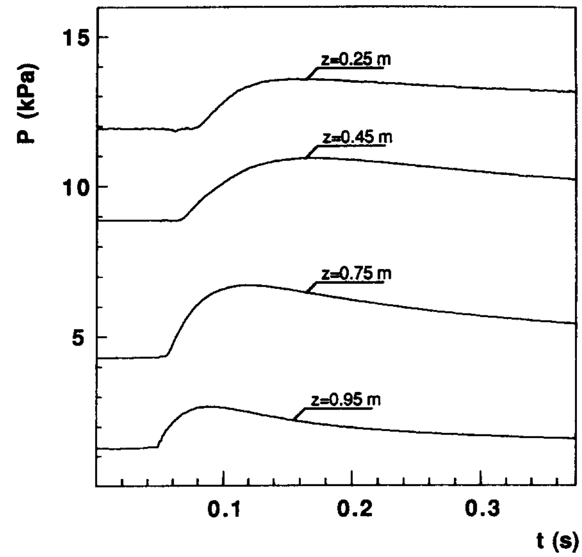

Figure 6. 0.10 m i.d. column. Pressure–time response to a step compression of the bed surface at four heights above the distributor.

(iii) At $U \geqslant U_{mb}$, propagation velocities range between a minimum of 15 m/s for bubble chain injection to a maximum of 22 m/s for step compression of the bed surface
(iv) For the same bed operating conditions different types of disturbances give values of the propagation velocities close to each other.

The comparison between velocities reported previously (table 1) and the values of c given in tables 2 and 3 shows that they all fall in the order of magnitude of 10 m/s.

Time delays related to the detection of pressure signals above and below the point of injection of a freely rising bubble in the 0.1 m i.d. column are reported in figure 11 as a function of the distance from the gas distributor. The disturbance generates two waves that depart from the origin (0.8 m from the base of the bed) and move in opposite directions. The slopes of the two straight lines departing from the disturbance point being equal but opposite, the velocity of propagation, i.e. the absolute value of c, is the same in both directions.

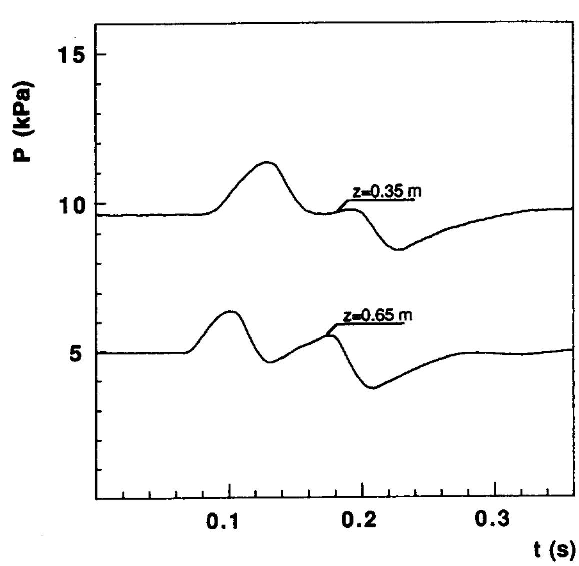

Figure 7. 0.10 m i.d. column. Pressure–time response to the injection of a freely rising bubble at two heights above the distributor.

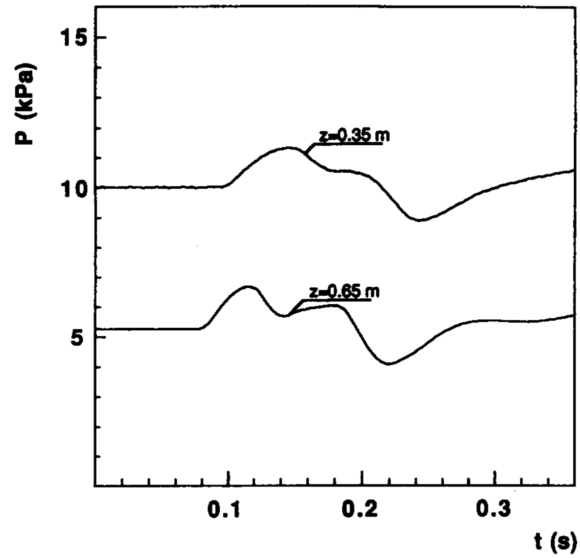

Figure 8. 0.10 m i.d. column. Pressure–time response to the injection of a captive bubble at two heights above the distributor.

Amplitude of Pressure Disturbances

Amplitudes (A_p) of pressure disturbances originated by jet discharge in the 0.35 m i.d. column are shown in figure 12(a,b) for different values of u_j and U. Figure 12(a) reports A_p for pressure signals on the axis and at the wall of the column; figure 12(b) shows A_p for pressure signals at two different heights above the gas distributor. The amplitudes of the signals are larger, the higher the gas velocity at the nozzle and the greater the fluidization velocity. They are attenuated in the direction of the propagation of the disturbance, decaying to 50–60% of their value after about 0.2 m in the radial direction [figure 12(a)] and to 60–80% of their value after 0.12 m in the vertical direction [figure 12(b)].

Amplitudes (A_s) measured at different distances from the distributor of the 0.1 m i.d. column in the experimental configuration of figure 3(a) are shown in figure 13(a). The lower the bed voidage, the lower the pressure increase (A_s) induced by the disturbance. As disturbances move away from the bed free surface where the compression originated, amplitudes of pressure signals first increase, reach a maximum, and then decrease. Amplitudes (A_s) measured at different distances from the distributor in the case of the injection of a freely rising bubble [figure 3(b)] and of a captive bubble [figure 3(c)] are reported in figure 13(b, c). Again, lower pressure increases

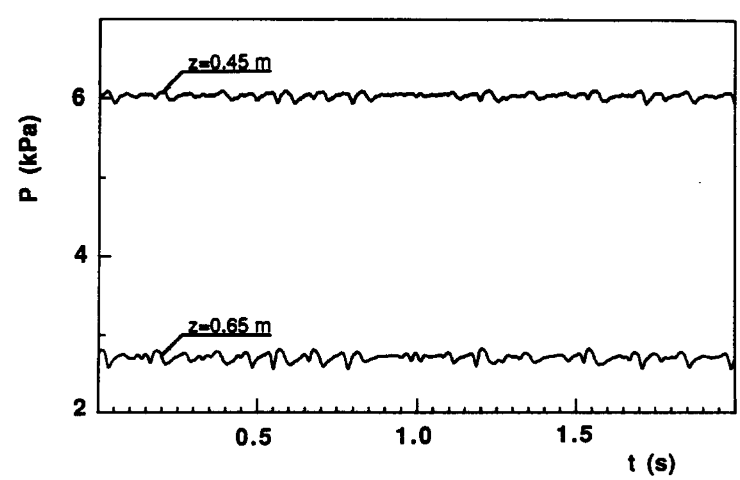

Figure 9. 0.10 m i.d. column. Pressure–time response to bubble chain injection at two heights above the distributor.

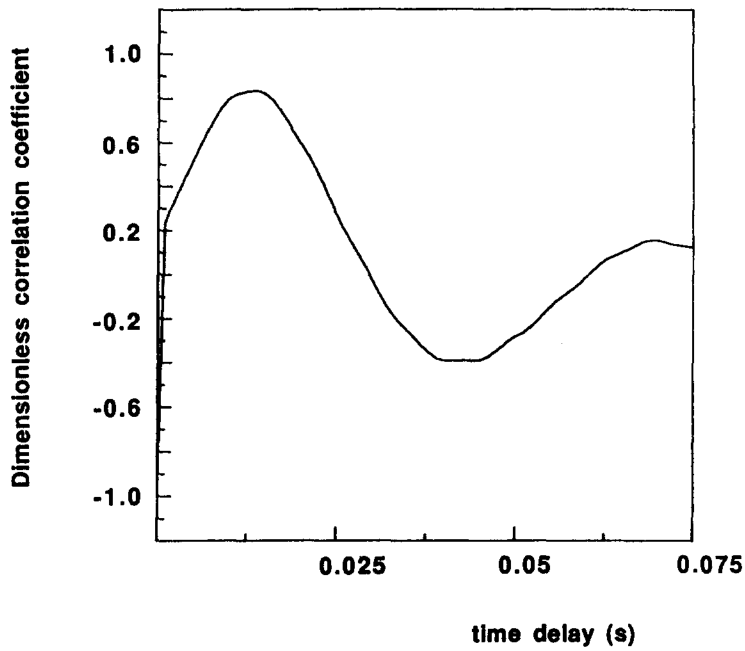

Figure 10. 0.10 m i.d. column. Cross-correlation diagram of the pressure profiles in figure 9.

(A_s) are found with lower bed voidages. Signal attenuation or growth can both occur, depending on the actual value of ϵ. These findings are in substantial agreement with the results given in figure 13(a).

4. COMPARISON WITH AVAILABLE THEORIES AND DISCUSSION

Propagation Velocities of Pressure Disturbances

The experimental results in figure 11 suggest that pressure disturbances behave like dynamic waves moving through the bed. In particular, according to wave theory (Lighthill 1978; Wallis 1969), a one-dimensional dynamic wave propagates in both directions with velocity $\pm c$ with respect to the mean fluid velocity.

Available theories on dynamic waves in solid–gas dispersions are borrowed from continuous mechanics of homogeneous systems, where the general equation for the velocity of propagation in fluids is

$$c_0 = \sqrt{\frac{E_f}{\rho_f}}, \qquad [1]$$

E_f being the absolute value of the bulk elasticity modulus and ρ_f the density of the fluid. Equation [1] has been modified to account for the peculiarities of the two-phase flow. Modifications fall into two categories: the first leads to a pseudo-homogeneous model; the second to a separated phase flow model.

Table 3. Propagation velocities (m/s) measured with the 0.1 m i.d. experimental apparatus ($U_{mf} = 0.021$ m/s; $U_{mb} = 0.026$ m/s)

U[m/s]:	0.021	0.023	0.025	0.026	0.028	0.032	0.035	0.042	0.049
ϵ:	0.387	0.390	0.396	0.406	—	—	—	—	—
0.10 m i.d. column; bed step compression	30.0	26.0	22.0	21.0	22.0	21.0	19.7	20.0	18.2
0.10 m i.d. column; single bubble injection, injected gas volume 0.125×10^{-3} Nm^3	22.3	18.4	18.9	19.0	19.2	18.7	19.0	19.0	18.5
0.10 m i.d. column; single bubble injection, injected gas volume 0.350×10^{-3} Nm^3	21.4	21.4	23.0	19.5	19.1	19.1	19.3	19.0	18.8
0.10 m i.d. column; captive bubble injection, injected gas volume 0.125×10^{-3} Nm^3	28.6	25.0	18.2	17.8	17.8	17.8	17.5	17.9	17.7
0.10 m i.d. column; bubble chain	—	—	—	15.5	—	14.6	—	15.0	—

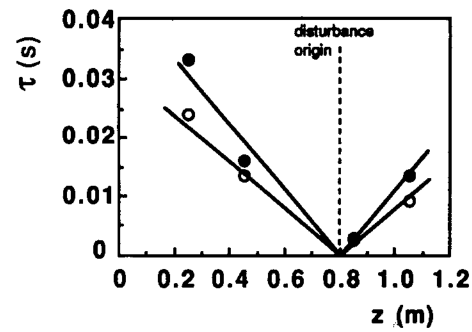

Figure 11. 0.10 m i.d. column. Time delays determined from pressure–time records above and below the point of injection of a freely rising bubble at minimum fluidization (○) and at minimum bubbling (●).

Pseudo-homogeneous model

The basic assumptions of the model are: (i) zero relative velocity between gas and solids; and (ii) the two-phase mixture acts as a fluid that obeys the usual equations of single-component flow provided suitable average properties of the mixture are adopted. Equations proposed by Wallis (1969, chap. 2) and Roy *et al.* (1990) are related to this model. These two equations are substantially the same. When considering that under the conditions of interest in this study

$$\rho_f c_0 \ll \rho_p c_p \quad \text{and} \quad \rho_f \ll \rho_p, \qquad [2]$$

where ρ_p is the solids density and c_p is the dynamic wave velocity in the solids, Wallis's (1969) equation gives:

$$c = c_0\sqrt{\frac{\rho_f}{\rho_p\epsilon(1-\epsilon)}} = \sqrt{\frac{E_f}{\rho_p\epsilon(1-\epsilon)}}. \qquad [3]$$

The comparison of [3] with [1] shows that the elasticity modulus embodied in the propagation velocity equation of the pseudo-homogeneous model is the same as that of the fluid, i.e. $10^5\ N/m^2$ for air at standard conditions.

Separated phase flow model

This model assumes that: (i) the gas is incompressible; (ii) there is a significant relative velocity between the gas and solids; and (iii) there is interaction between the gas and solid phase and within the solid phase because of particle-to-particle collisions. Equations proposed by Wallis (1969,

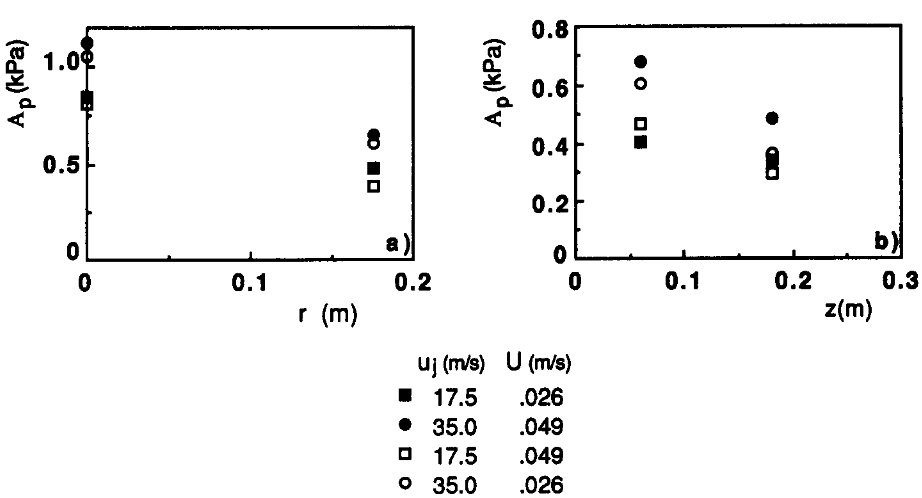

Figure 12. 0.35 m i.d. column. Radial (a) and vertical (b) amplitude variation of pressure–time signals induced by gas discharge.

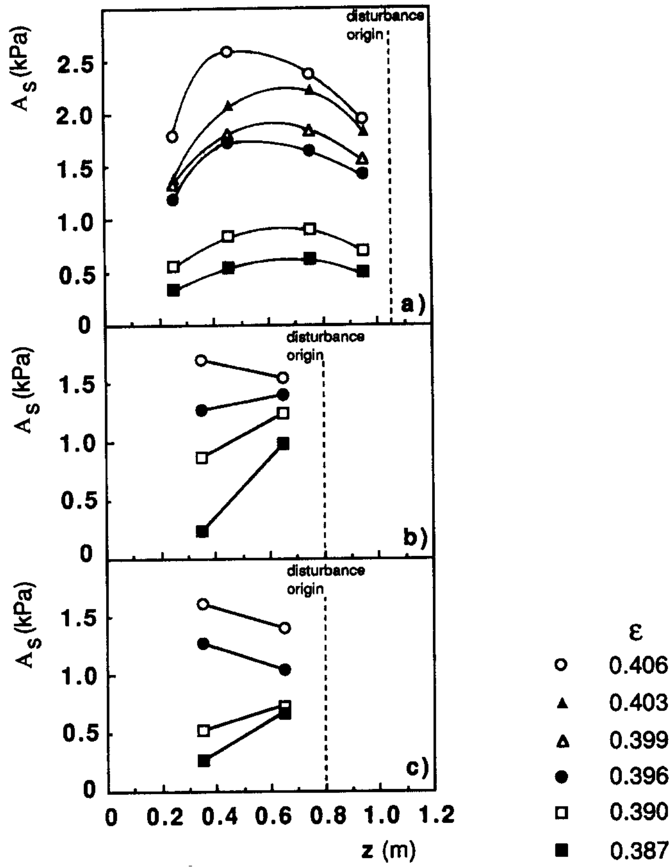

Figure 13. 0.10 m i.d. column. Amplitudes of pressure–time signals for different disturbances imparted to the bed: (a) compression of bed free surface; (b) injection of a freely rising bubble; (c) injection of a captive bubble.

chap. 6) and Fanucci *et al.* (1981), which are substantially the same, are related to this model. In particular, Fanucci *et al.*'s (1981) equation is

$$c = \sqrt{-(v_s)^2 \frac{(1-\epsilon)\rho_f}{\epsilon \rho_p} - (1-\epsilon)\frac{E_b}{\rho_p}}, \qquad [4]$$

where v_s is the gas–solid particle relative velocity and E_b, which is inherently negative, is the bulk elasticity modulus of the dispersed solid phase. In spite of the incompressibility of both gas and particles a finite value of E_b is originated by voidage change in the gas–solid assemblage.

Equations for the dynamic wave velocity c of the suspension based on the separated phase flow model have been developed by Verloop & Heertjes (1970), Mutsers & Rietema (1977) and Foscolo & Gibilaro (1984) in the framework of studies directed to verify the Wallis criterion on the onset of bubbling in bubble-free fluidized beds. Poletto & Massimilla (1992) have reexamined experimental results on the onset of bubbling in homogeneous beds in the light of theories proposed by the above authors and of Batchelor's (1988) theory. They found that in any case the elasticity modulus $-E_b$ was in the range 10–100 N/m^2.

Values of c predicted from [3] are in fair agreement with those obtained in this work. However, the dependence of c on ϵ expressed by [3] is not satisfactory. For instance, when ϵ changes from ϵ_{mb} to ϵ_{mf}, this equation predicts a very weak variation of c between 13.1 and 13.3 m/s, whereas the experimental values range between 20 and 30 m/s (table 3).

Values of c predicted by [4] are much lower than those found experimentally. They vary between 0.04 and 0.12 m/s for $-E_b = 10$ or 100 N/m^2 in [4]; those obtained from the equations of Verloop & Heertjes (1970) and Foscolo & Gibilaro (1984), and from [4] with Mutsers & Rietema (1977) estimate of E_b, are in the same order of magnitude.

Summarizing the above results, it appears that under all the experimental configurations in which the two columns of figures 1 and 2 have been operated in this work (gas jetting, bubble chain, freely rising and captive bubble injection, top surface compression) the elastic modulus of the fluid should be called in to justify the propagation velocity of disturbances. On the contrary, the interpretation of the onset of bubbling on the basis of the studies of Wallis (1962), Verloop & Heertjes (1970), Foscolo & Gibilaro (1984) and Piepers & Rietema (1989) calls in the elastic modulus of the assemblage of solid particles immersed in the fluid.

Amplitude of Pressure Disturbances

The amplitudes (A_p) measured in the 0.35 m i.d. column (figure 12) respond to the expectation that the disturbance decays with the distance from the origin, assuming that the source of the disturbance is in the proximity of the nozzle.

The decay of the amplitudes (A_s) measured in the 0.10 m i.d. column with the distance from the source of the disturbance (figure 13) may be expected as an effect of the attenuation of dynamic waves through two-phase systems, e.g. by the viscous and thermal dissipation mechanisms considered by Epstein & Carhart (1953) in their analysis for pseudo-homogeneous systems. Instead, it is difficult to explain the increase in A_s downstream from the disturbance source in the light of such theoretical considerations.

5. CONCLUSIONS

The response to disturbances induced in a small-scale bed suggests that pressure disturbances move through fluidized beds as dynamic waves.

Numerical values of the propagation velocities of pressure disturbances associated with gas jetting in a relatively large fluidized bed are close to those found in experiments carried out by inducing different types of disturbances in beds contained in a test tube of small diameter. They are of the order of 10 m/s.

Wave propagation velocities are in fair agreement with those predicted by the "pseudo-homogeneous" model using the fluid elasticity modulus as the elasticity modulus of the medium. These velocities are 2 orders of magnitude larger than those predicted by the "separated phase flow" model when the elasticity moduli of the dispersed solid particles, such as those obtained from experiments on incipient bubbling, are used in the wave velocity equations.

REFERENCES

BATCHELOR, G. K. 1988 A new theory of the instability of a uniform fluidized bed. *J. Fluid Mech.* **193,** 75–110.

EL-KAISSY, M. M. & HOMSY, G. M. 1976 Instability waves and the origin of bubbles in fluidized beds. *Int. J. Multiphase Flow* **2,** 379–395.

EPSTEIN, P. S. & CARHART, R. R. 1953 The absorption of sound in suspensions and emulsions *J. Acoust. Soc. Am.* **25,** 553–565.

FAN, L. T., THO-CHING, HO, HIRAOKA, S. & WALAWENDER, W. P. 1981 Pressure fluctuation in a fluidized bed. *AIChE Jl* **27,** 388–396.

FANUCCI, J. B., NESS, N & YEN, R. H. 1981 Structure of shock waves in gas particulate fluidized beds. *Phys. Fluids* **24,** 1944–1954.

FILLA, M., MASSIMILLA, L., MUSMARRA, D. & VACCARO, S. 1986 Pressure fluctuations associated with gas injection in fluidized beds. In *Fluidization V* (Edited by OSTERGAARD, K. & SORENSON, A.), pp. 71–78. Engineering Foundation, New York.

FOSCOLO, P. U. & GIBILARO, L. G. 1984 A fully predictive criterion for the transition between particulate and aggregate fluidization. *Chem. Engng Sci.* **39,** 1667–1675.

LIGHTHILL, J. 1978 *Waves in Fluids*. Cambridge Univ. Press, Cambs.

LIRAG, R. C. & LITTMAN, H. 1971 Statistical study of pressure fluctuations in a fluidized bed. *AIChE Symp. Ser.* **67,** 11–22.

MASSIMILLA, L. 1985 Gas jets in fluidized beds. In *Fluidization*, 2nd edn (Edited by DAVIDSON, J. F., CLIFT, R. & HARRISON, D.), pp. 133–172. Academic Press, London.

POLETTO, M. & MASSIMILLA, L. 1992 Stability analysis of uniformly fluidized beds in terms of the elastic modulus of the dispersed phase. *Powder Technol.* In press.

MUTSERS, S. P. M. & RIETEMA, K. 1977 The effect of interparticle forces on the expansion of a homogeneous gas-fluidized bed. *Powder Technol.* **18,** 238–248.

PIEPERS, H. W. & RIETEMA, K. 1989 Effects of pressure and type of gas on gas–solid fluidization behaviour. In *Fluidization VI* (Edited by GRACE, J. R., SHEMILT, L. W. & BERGOUGNOU, M. A.), pp. 203–210. Engineering Foundation, New York.

ROY, R., DAVIDSON, J. F. & TUPONOGOV, V. G. 1990 The velocity of sound in fluidised beds. *Chem. Engng Sci.* **45,** 3233–3245.

VACCARO, S., MUSMARRA, D., FILLA, M. & MASSIMILLA, L. 1989 Diagnostic of gas injection in fluidized beds by pressure signal analysis. In *Fluidization VI* (Edited by GRACE, J. R., SHEMILT, L. W. & BERGOUGNOU, M. A.), pp. 245–252. Engineering Foundation, New York.

VERLOOP, J. & HEERTJES, P. M. 1970 Shock waves as a criterion for transition from homogeneous to heterogeneous fluidization. *Chem. Engng Sci.* **25,** 825–832.

WALLIS, G. B. 1962 One dimensional waves in two-component flow. Report No R162, Atomic Energy Establishment, Winfrith, U.K.

WALLIS, G. B. 1969 *One Dimensional Two Phase Flow.* McGraw-Hill, London.